Doc Ophthalmol (2021) 143:53–60
https://doi.org/10.1007/s10633-021-09822-2

ORIGINAL RESEARCH ARTICLE

Pseudorandom full-field electroretinograms reflect different light adaptation mechanisms

Juliana Bizerra Assis · Alódia Brasil · Terezinha Medeiros Gonçalves Loureiro · Veronica Gabriela Ribeiro da Silva · Anderson Manoel Herculano · Dora Fix Ventura · Luiz Carlos Lima Silveira · Jan Kremers · Givago Silva Souza

Received: 26 June 2020 / Accepted: 20 January 2021 / Published online: 19 February 2021

Abstract

Purpose To investigate the magnitude and time course of pseudorandom ffERG during light adaptation.

Methods Ten healthy subjects (26 ± 10.1 years) underwent 20 min of dark adaptation, and then the ffERG was evoked by pseudorandom flash sequences (4 ms per flash, 3 cd.s/m^2) driven by m-sequences (2^{10}–1 stimulus steps) using Veris Science software and a Ganzfeld dome over a constant field of light adaptation (30 cd/m^2). The base period of the m-sequence was 50 ms. Each stimulation sequence lasting 40 s was repeated at 0, 5, 10, 15 and 20 min of light adaptation. Relative amplitude and latency (corrected by values found at 0 min) of the three components (N1, P1, and N2) of first-order (K_1) and first slice of the second-order ($K_{2,1}$) kernel at 5 time points were evaluated. An exponential model was fitted to the mean amplitude and latency data as a function of the light adaptation duration to estimate the time course (τ) of the light adaptation for each component. Repeated one-way ANOVA followed by Tukey post-test was applied to the amplitude and latency data, considering significant values of $p < 0.05$.

Results Regarding the K_1 ffERG, N1 K_1, P1 K_1, and N2 K_1 presented an amplitude increase as a function of the light adaptation (N1 K_1 τ value = 2.66 min ± 4.2; P1 K_1 τ value = 2.69 min ± 2.10; and N2 K_1 τ value = 3.49 min ± 2.96). P1 K_1 and N2 K_1 implicit time changed as a function of the light adaptation duration (P1 K_1 τ value = 3.61 min ± 5.2; N2 K_1 τ value = 3.25 min ± 4.8). N1 K_1 had small implicit time changes during the light adaptation. All the $K_{2,1}$ components also had nonsignificant changes in amplitude and implicit time during the light adaptation.

Conclusions Pseudorandom ffERGs showed different mechanisms of adaptation to retinal light. Our results suggest that K_1 ffERG is generated by retinal mechanisms with intermediate- to long-term light

Luiz Carlos Lima Silveira: Deceased

J. B. Assis · T. M. G. Loureiro · V. G. R. da Silva · A. M. Herculano · L. C. L. Silveira · G. S. Souza
Instituto de Ciências Biológicas, Universidade Federal do Pará, Belém, Pará, Brazil

A. Brasil (✉) · L. C. L. Silveira · G. S. Souza
Núcleo de Medicina Tropical, Universidade Federal do Pará, Belém, Pará, Brazil
e-mail: alodiabrasil@ufpa.br

A. Brasil
Faculdade de Nutrição, Instituto de Ciências da Saúde, Universidade Federal do Pará, Av. Generalíssimo Deodoro 92, Umarizal, Belém, Pará 66055-240, Brazil

D. F. Ventura
Instituto de Psicologia, Universidade de São Paulo, São Paulo, Brazil

J. Kremers
Department of Ophthalmology, University Hospital Erlangen, Erlangen, Germany

adaptation, while $K_{2.1}$ ffERG is generated by retinal mechanism with fast light adaptation course.

Keywords Visual electrophysiology · Full-field ERG · Light adaptation · Retina · Pseudorandom stimulation

Introduction

Visual adaptation is a readjustment of response and sensitivity of the visual system after a change in overall luminance and/or chromaticity. One of these readjustments appears in the electroretinogram (ERG) when an observer is exposed to light after a period of dark adaptation [1–6] that is characterized by an increase in amplitude after the background light is switched on. This process may take several minutes [1–3, 7–10].

Different mechanisms have been proposed to explain this phenomenon. Kondo et al. [8] recorded multifocal ERGs to study the effects of light adaptation at different retinal eccentricities. They observed that in the central retina, the rate of change in the ERG amplitude was slower than that in the peripheral retina, indicating that rod signals may influence the rate of light adaptation in cone-driven responses. The notion that rods may play a role was recently supported by results from measurements in mice in which it was found that the increase in cone-driven ERGs was substantially different in mice without functional rods. [11]. However, Peachey et al. [12] showed that the ERG amplitude growth during light adaptation was also present in a patient with congenital stationary night blindness with no measurable rod-driven responses. Armington and Biersdorf [1] suggested that the electrooculogram (EOG) increases in parallel with the ERG during light adaptation. Therefore, they proposed that the pigment epithelium, which is the generator of the EOG, is responsible for the ERG changes. However, the time course of amplitude changes differed in the EOG and the ERG. More importantly, the ERG amplitude growth during light adaptation occurs even in isolated frog retinae that are detached from the retinal pigment epithelium [13, 14]. McAnany and Nolan [9] recorded ERGs to 31 Hz sinusoidal modulation. They found that the fundamental, second, and third harmonics of the response had different time courses during light adaptation, suggesting that the ERG changes during light adaptation are the result of different mechanisms. Brasil et al. [10] used sinusoidal L- and M-cone isolating stimuli in addition to luminance and isoluminant chromatic stimuli to study light adaptation in the ERG. They observed that the light adaptation process reflected mainly the changes in the luminance channel.

There is evidence that the first- and second-order kernels of the multifocal ERG are generated by different retinal circuitries [15–17]. The first-order kernel (K_1) represents the direct response to the stimulus flash (linear response), and the contribution of the nonlinear response contribution is small and depends on the stimulus step interval. The first slice of the second-order kernel ($K_{2.1}$) represents the time interaction of responses elicited by two consecutive stimuli and is dependent on the presence of nonlinear mechanisms [18] and receives contribution of nonlinear mechanisms. Similar to adaptation, $K_{2.1}$ represents a time-shifted response adjustment. It is unclear whether light adaptation has similar effects on the cellular mechanisms underlying K_1 and $K_{2.1}$. In the present study, we explore the changes in K_1 and $K_{2.1}$ during light adaptation. We therefore measured the ERG responses to pseudorandom sequences of full-field flashes at different times during light adaptation to obtain full-field K_1 and $K_{2.1}$ responses and to estimate their time courses during light adaptation.

Methods

Subjects

Ten healthy subjects between 19 and 52 years of age (mean ± SD: 26 ± 10.1 years) participated in the present study. None of the subjects had a history of ophthalmological, neurological, or systemic disease that might have affected the electrophysiological responses. The procedures were in agreement with the tenets of Helsinki and were approved by the ethics committee for research with humans of the Tropical Medicine Institute from Federal University of Pará, Brazil (report # 007/2011).

The ERGs were recorded from a randomly chosen eye. The pupils were dilated through topical administration of a drop of mydriatic (tropicamide 1%). A corneal DTL fiber was the active electrode, and

surface electrodes placed at the ipsilateral temporal canthus and the forehead were reference and ground electrodes, respectively.

Stimulation

The Veris Science software (ElectroDiagnostic Imaging, EDI, CA) controlled a 12-bit full-field stimulator (diameter of 38 cm) to present pseudorandom sequences of flashes. A 4-colored light emitting diode (LED) array was used for visible white background illumination and flashes (Table 1). Flashes with 4 ms duration and 3 cd. s/m^2 of strength were presented on a 30 cd/m^2 (ca. 1500 td) adapting background. The flashes were presented using m-sequences (2^{10}–1 stimulus steps) with a base period of 50 ms.

Recording settings

The electrode impedance was kept below 5 kΩ. The signals were amplified 50,000 times and digitized with a sampling rate of 2 kHz. The recordings were band-pass-filtered with 10 and 300 Hz cutoff frequencies.

Experimental procedures

After the electrodes were placed, each subject was dark-adapted for 20 min in a dark room and with closed eyes. They were then requested to open their eyes and were exposed to steady adaptation background of 30 cd/m^2 of the stimulator. Directly at the beginning of the exposure, a pseudorandom flash sequence was presented for 40 s and the ERG was recorded. The measurements were repeated 5, 10, 15, and 20 min after the onset of the light adaptation.

Data analysis

The Veris Science software was used to extract the kernels of the flash responses by cross-correlations between stimulus and measured signals. We extracted the first-order kernel (K_1) and the first slice of the second-order kernel ($K_{2.1}$) and measured the amplitude of the different components. We defined three components in the first-order kernels: N1 K_1, P1 K_1, and N2 K_1 (Fig. 1). Similarly, three components were defined in the second-order kernels: N1 $K_{2.1}$, P1 $K_{2.1}$, and N2 $K_{2.1}$. We averaged the data points after digitization during the first 5 ms after flash onset of the individual final waveform of each ERG kernel to represent the baseline of the response. During this period, a significant ERG signal is not present. The amplitudes of the N1 and N2 components were the voltage differences between baseline and the trough between 10 and 25 ms and between 35 and 50 ms, respectively. P1 amplitudes were the voltage difference between the baseline and the peak between 20 and 35 ms. The implicit time of each component was the time interval between the onset of a flash and ERG components' peaks or troughs.

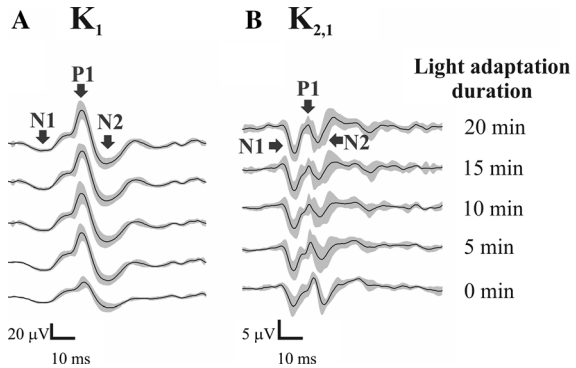

Fig. 1 Averaged ERG waveforms from 10 subjects during durations of light adaptation. **a** First-order kernels, K1. **b** First slice of the second-order kernels, K2.1. For each response, we measured the amplitude of the first three components named here as N1, P1, and N2 at 0, 5, 15, and 20 min of light adaptation. Shaded areas represent the mean ± SD

An exponential function (Eq. 1) was fitted to the ERG amplitude (normalized to the amplitude at $t = 0$)

Table 1 Contribution of the LEDs to the stimulus and background light intensity

LED	Dominant wavelength (nm)	Contribution for the flash light (cd s/m^2)	Contribution for background light
Red	627	0.5962	3.2736
Green	530	2.3292	26.2022
Blue	470	0.0753	0.4792
Amber	590	0	0

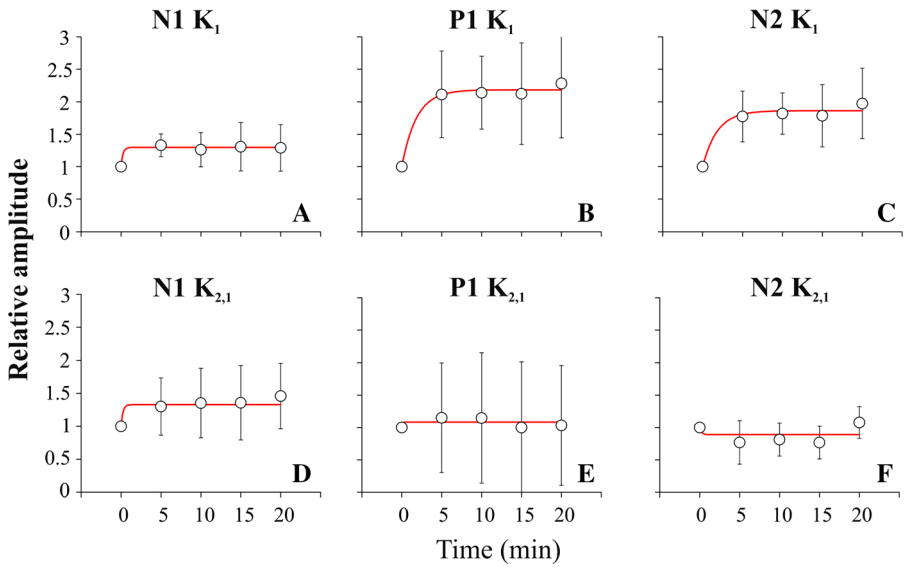

Fig. 2 Mean relative amplitude as a function of light adaptation duration for K1 components (upper row), and K2.1 components (lower row). Circles represent the mean amplitude values, error bars represent the standard deviation, and the red curves are the best fits of the model, described by Eq. (1), to the data. **a** N1 K_1, **b** P1 K_1, **c** N2 K_1, **d** N1 $K_{2.1}$, **e** P1 $K_{2.1}$, **f** N2 $K_{2.1}$

and the change in implicit time (relative to the one at $t = 0$) vs adaptation time [10].

$$y = yo + a \times e^{-t/\tau} \quad (1)$$

where y is the normalized amplitude or implicit time change of the model at time t of the light adaptation, yo is the normalized amplitude or implicit time difference relative to the values at onset of light adaptation, a describes the maximal normalized amplitude or implicit time changes, and τ is the time constant (semi-saturation constant) of light adaptation and indicates the time at which $a/2$ was reached. Parameters a and τ were free parameters in the fitting procedure. We fitted individual amplitude and implicit time data to estimate individual model parameters. These parameters were used in statistical analyses. We also fitted the model to the averaged data to visualize the goodness of fits in Figs. 2 and 3.

We used repeated one-way ANOVA with Geisser–Greenhouse correction and followed by a Tukey's multiple comparison test to compare the relative amplitude and implicit times of the different time points after 0 min. The significance level of 0.05 was corrected for multiple comparisons. GraphPad Prism 8 (GraphPad software, San Diego, CA) was used for the statistical analysis.

Results

Pseudorandom full-field ERG waveforms

Figure 1 shows the averaged full-field ERG K_1 and $K_{2.1}$ waveforms from 10 subjects recorded at different times after onset of the light adaptation. The gray areas identify the mean ± 1 SD. Clearly, the K_1 response increased with increasing adaptation time. However, the changes after 5 min of adaptation are substantially smaller than the changes up to 5 min after onset of the adaptation light. No systematic changes can be observed in the $K_{2.1}$ response.

Pseudorandom full-field ERG normalized amplitude as a function of duration of light adaptation

We measured the amplitudes of the three different K_1 and $K_{2.1}$ ERG components and normalized them to the amplitude at $t = 0$ s. Their mean normalized amplitude values (± 1 SD) are displayed in Fig. 2 as a function of adaptation time, and the red curves display the fits of Eq. (1) to the averaged data. N1 K_1, P1 K_1, and N2 K_1 grew after 0 min, but there was no significant growth along the light adaptation period (N1 K_1: F(1.57,

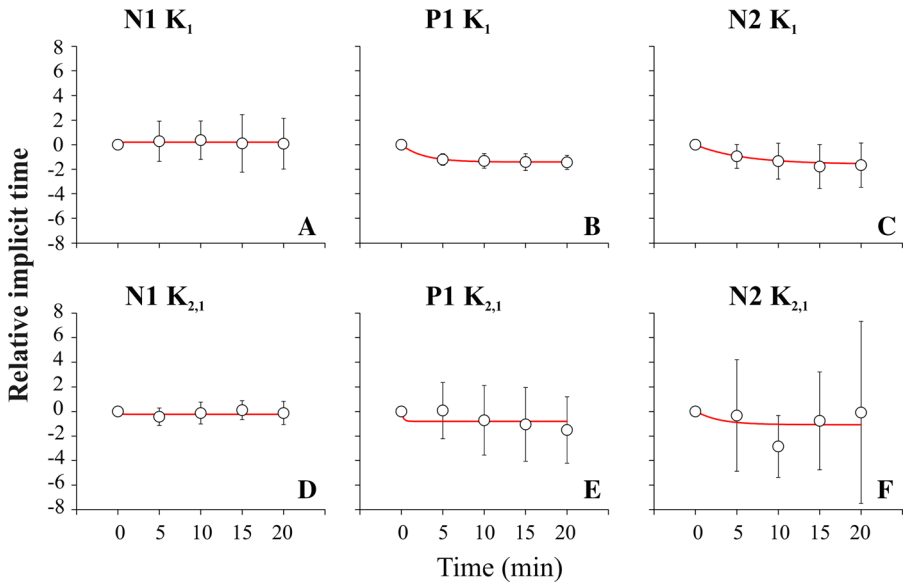

Fig. 3 Mean relative implicit time as a function of light adaptation duration for K1 components (upper row), and K2.1 components (lower row). Circles represent the mean implicit time values, error bars represent the standard deviation, and the red curves are the best fits of the model, described by Eq. (1), to the data. **a** N1 K_1, **b** P1 K_1, **c** N2 K_1, **d** N1 $K_{2,1}$, **e** P1 $K_{2,1}$, and **f** N2 $K_{2,1}$

14.21) = 0.26, p = 0.71; P1 K_1: F(1.583, 12.66) = 1.06, p = 0.53; N2 K_1: F(2.02, 16.2) = 1.2, $p < 0.32$). For N1 K_1, P1 K_1 and N2 K_1, the amplitude growth during light adaptation had τ values of 2.66 ± 4.21, 2.69 ± 2.10 and 3.49 ± 2.96, respectively. All the $K_{2,1}$ components had nonsignificant changes during the light adaptation (N1 $K_{2.1}$: F(2.24, 20.19) = 2.02, p = 0.15; P1 $K_{2.1}$: F(1.98, 17.82) = 1.46, p = 0.26; N2 $K_{2.1}$: F(2.03, 18.23) = 1.98, p = 0.17).

We measured the implicit time changes of the K_1 and $K_{2.1}$ ERG components. Their mean values are displayed in Fig. 3 as a function of the time after onset of the adapting background, and the curves represent the fits of Eq. (1) to the data. The P1 K1 and N2 K1 fits returned a values of − 1.53 ± 0.69 and − 1.60 ± 1.85, respectively, and τ values of 3.61 ± 5.24 and 3.25 ± 4.79, respectively. N1 K_1 had small variation of the implicit time as a function of the time. For all the $K_{2.1}$ components, there were no systematic changes of the implicit time, and no significant differences were observed.

Discussion

We found that K_1 and $K_{2.1}$ ERG had different responses to light adaptation and attribute these differences to mediation of different mechanisms. Our findings confirmed previous findings about the influence of the light adaptation duration on the K_1 ERG [8], and extended the knowledge about light adaptation of ERGs, showing that $K_{2.1}$ ERG has either small or no influence from the light adaptation time course. We showed that the amplitudes of the K_1 ERG components grew and the implicit times of some components changed. There were no significant changes in the $K_{2.1}$ ERG components during the light adaptation period. Probably, no overlap occurs between N2 K_1 and P1 $K_{2,1}$ because if a substantial overlap were to occur, we would have expected that the amplitude of the $K_{2,1}$ ERG component would have changed as a function of the adaptation time, which is not the case.

K_1 ERG represents the linear response of the visual system to the flash stimulus, and it is an approximation of the conventional ERG waveforms elicited by full-field stimulation. In contrast, the second-order kernel represents a nonlinear response of the visual system to preceding stimulation [18, 19]. Although we have applied a longer base period than most previous studies, we consider that our general findings are comparable to them, because no significative difference in retinal origins of mfERG has been reported in

investigations that used slow- and fast-sequence mfERG [15].

The retinal contributions to the ERG depend on the retinal illuminance. In dark-adapted conditions, the retinal signals are generated by rods and transmitted to rod ON-bipolar cells and horizontal cells, while in light-adapted conditions the retinal signals are driven by cones [20]. The cone signals can be modulated by electrical coupling between rods and cones, which may change during light adaptation [21]. The cone signals are transmitted to the outer plexiform layer to ON- and OFF-bipolar cells and horizontal cells [22, 23]. Horizontal cells have a role of negative feedback on cone photoreceptor that modulates dynamic ranges of retinal bipolar cells so that a brighter light flash is required to elicit bipolar cell response when it is exposed to brighter background [24]. Several studies have reported light adaptation changes in the conventional full-field ERG components similar to those observed in our K1 ERGs [1–6, 25, 26]. Kondo et al. [8] offered the first description that pseudorandom ERGs also show light adaptation changes. They measured multifocal ERGs and evaluated the light adaptation changes of the first-order kernels at different visual field eccentricities. In the central retina, the rate of change of mfERG amplitude during light adaptation was smaller than that in the peripheral retina. Kondo et al. [8] suggested that rods could exert inhibition on the cones whose response was reduced due to light adaptation. The current study is the first to report the influence of light adaptation on the $K_{2.1}$ ERG.

The novel finding of the present study is the description of the adaptation kinetics of ERG components to pseudorandom stimuli, especially those of the $K_{2,1}$. A possible explanation for the differences observed between K_1 and $K_{2.1}$ ERGs may be that their underlying cellular mechanisms are different. These cellular mechanisms have been investigated using pharmacological blocking in the retina of non-human primates or other mammals [16, 17, 27, 28]. Pharmacological blockade of the sodium-based action potential in ganglion cells and some amacrine cells (inner retina) by tetrodotoxin (TTX) resulted in an amplitude increase of the K_1 ERG indicating a major contribution of the outer retina to the K_1 components [16, 17, 28]. Similar to neurons in the outer retina, K_1 components of our experiments show systematic alterations during light adaptation. Pharmacological blockade of inner retinal neurons led to a strong decrease of $K_{2,1}$ ERG components' amplitude, indicating that these cells are the main contributors to the $K_{2,1}$ [16, 17, 28]. Considering the inner retinal origin of $K_{2,1}$ ERG, it can be expected that the $K_{2,1}$ ERG changes in a similar way as the inner retinal neurons. Retinal ganglion cells adapt quickly with time constants in the order of seconds [28], which could explain that the $K_{2.1}$ did not change significantly during light adaptation, because the time course of inner retinal adaptation is too fast to be detected by the longer-lasting measurements described here.

The glutamate analogs, such as L-2-amino-4-phosphonobutyric acid (APB) and cis-2,3 piperidine dicarboxylic acid (PDA), have been used to block the transmission of the photoreceptor to the bipolar cells [29, 30]. PDA blocks the transmission to the OFF-bipolar, while APB blocks the transmission to the ON-bipolar cells [30, 31], and the use of both glutamates analogs together isolates the photoreceptor contribution to the recording [15, 16]. It was found that the K_1 ERG was largely suppressed by blocking all bipolar cells such as occur to the conventional full-field ERG. Because of the similarity between light adaptation time course and effects of pharmacological blockade, the K_1 ERG and the single-flash full-field ERG probably share the same light adaptation mechanism in the outer retina.

Our results reinforce the hypothesis of the preferential contribution of the outer and inner retina to the K_1 and $K_{2.1}$ ERGs, respectively. The biggest advantage of the use of single-flash full-field pseudorandom ERGs is that they allow studying different retinal light adaptation mechanisms (originating in outer and inner retinal neurons).

Acknowledgements This research was supported by the following grants: Conselho Nacional de Desenvolvimento Científico e Tecnológico-CNPq- Programa de Apoio aos Núcleos de Excelência- PRONEX / Fundação Amazônia de Amparo a Estudos e Pesquisa do Pará-FAPESPA #316,799/2009; CNPq #486,545/2012-1, 431,748/2016-0; Financiadora de Estudos e Projetos -FINEP- Instituto Brasileiro de Neurociência -IBN Net #1723. JBA received CNPq fellowship for undergraduate student, VRS, Coordenação de Aperfeiçoamento de Pessoal de Nível Superior -CAPES fellowship for graduate students. AB received a Programa Nacional de Pós Doutorado-PNPD/CAPES post-doctoral fellowship. AH, DFV, and GSS are CNPq research fellows.

Compliance with ethical standards

Conflict of interest All authors certify that they have no affiliations with or involvement in any organization or entity with any financial interest (such as honoraria; educational grants; participation in speakers' bureaus; membership, employment, consultancies, stock ownership, or other equity interest; and expert testimony or patent-licensing arrangements) or non-financial interest (such as personal or professional relationships, affiliations, knowledge, or beliefs) in the subject matter or materials discussed in this manuscript.

Statement of human rights All procedures performed in studies involving human participants were in accordance with the ethical standards of the institutional and/or national research committee (Tropical Medicine Center Committee) and with the 1964 Declaration of Helsinki and its later amendments or comparable ethical standards.

Statement on the welfare animals No animals were used in this study.

Informed consent Informed consent was obtained from all individual participants included in the study.

References

1. Armington JC, Biersdorf WR (1958) Long-term light adaptation of the human electroretinogram. J Comp Physiol Psychol 51:1–5
2. Gouras P, MacKay CJ (1989) Growth in amplitude of the human cone electroretinogram with light adaptation. Invest Ophthalmol Vis Sci 30:625–630
3. Peachey NS, Alexander KR, Fishman GA, Derlacki DJ (1989) Properties of the human cone system electroretinogram during light adaptation. Appl Opt 28:1145–1150
4. Murayama K, Sieving PA (1992) Different rates of growth of monkey and human photopic a-, b-, and d-waves suggest two sites of ERG light adaptation. Clin Vis Sci 7:385–392
5. Benoit J, Lachapelle P (1995) Light adaptation of the human photopic oscillatory potentials: influence of the length of the dark adaptation period. Doc Ophthalmol 89:267–276
6. Alexander KR, Raghuram A, Rajagopalan AS (2006) Cone phototransduction and growth of the erg b-wave during light adaptation. Vision Res 46:3941–3948
7. Burian HM (1954) Electric responses of the human visual system. AMA Arch Ophthalmol 51:509–524
8. Kondo M, Miyake Y, Piao C-H, Tanikawa A, Horiguchi M, Terasaki H (1999) Amplitude increase of the multifocal electroretinogram during light adaptation. Invest Ophthalmol Vis Sci 40:2633–2637
9. McAnany JJ, Nolan PH (2014) Changes in the harmonic components of the flicker electroretinogram during light adaptation. Doc Ophthalmol 129:1–8
10. Brasil A, Tsai TI, da Silva SG, Herculano AM, Ventura DF, de Lima Silveira LC, Kremers J (2019) Pathway-specific light adaptation in human electroretinograms. J Vis 19:12. https://doi.org/10.1167/19.3.12
11. Bush RA, Tanikawa A, Zeng Y, Sieving PA (2019) Cone ERG changes during light adaptation in two all-cone mutant mice: implications for rod-cone pathway interactions. Invest Ophthalmol Vis Sci 60:3680–3688
12. Peachey NS, Fishman GA, Kilbride PE, Alexander KR, Keehan KM, Derlacki DJ (1990) A form of congenital stationary night blindness with apparent defect of rod phototransduction. Invest Ophthalmol Vis Sci 31:237–246
13. Hood DC (1972) Adaptational changes in the cone system of the isolated frog retina. Vision Res 12:875–888
14. Miyake Y, Horiguchi M, Ota I, Tokabayashi A (1988) Adaptational change in cone-mediated electroretinogram in human and carp. Neurosci Res Supp 8:S1-13
15. Rangaswamy NV, Hood DC, Frishman LJ (2003) Regional variations in local contributions to the primate photopic flash ERG: revealed using the slow-sequence mfERG. Invest Ophthalmol Vis Sci 44(7):3233–3247. https://doi.org/10.1167/iovs.03-0009
16. Hare WA, Ton H (2002) Effects of APB, PDA, and TTX on the first and second order responses of the multifocal ERG response in monkey. Doc Ophthalmol 105:189–222
17. Hood DC, Frishman LJ, Saszik S, Viswanathan S (2002) Retinal origins of the primate multifocal ERG: implications for the human response. Invest Ophthalmol Vis Sci 43:1673–1685
18. Sutter EE (2001) Imaging visual function with the multifocal m-sequence technique. Vision Res 41:1241–1255
19. Sutter EE (2000) The interpretation of multifocal binary kernels. Doc Ophthalmol 100:49–75
20. Boycott B, Dowling J, Kolb H (1969) Organization of the primate retina: light microscopy. Philosoph Trans Royal Soc London Series B, Biological Sciences 255(799):109–184
21. Raviola E, Gilula NB (1973) Gap junctions between photoreceptor cells in the vertebrate retina. Proc Natl Acad Sci USA 70(6):1677–1681. https://doi.org/10.1073/pnas.70.6.1677
22. Werblin FS, Dowling JE (1969) Organization of the retina of the mudpuppy, Necturus maculosus II. Intracellular recording. J Neurophysiol 32(3):339–355. https://doi.org/10.1152/jn.1969.32.3.339 (**PMID: 4306897**)
23. Kaneko A (1970) Physiological and morphological identification of horizontal, bipolar and amacrine cells in goldfish retina. J Physiol 207(3):623–633. https://doi.org/10.1113/jphysiol.1970.sp009084
24. Wu SM (1994) Synaptic transmission in the outer retina. Annu Rev Physiol 56:141–168. https://doi.org/10.1146/annurev.ph.56.030194.001041
25. Peachey NS, Alexander KR, Derlacki DJ, Fishman GA (1992) Light adaptation, rods, and the human cone flicker ERG. Visual Neurosci 8:145–150
26. Peachey NS, Arakawa K, Alexander KR, Marchese AL (1992) Rapid and slow changes in the human cone electroretinogram during light and dark adaptation. Vision Res 32:2049–2053
27. Horiguchi M, Suzuki S, Kondo M, Tanikawa A, Miyake Y (1998) Effect of glutamate analogues and inhibitory neurotransmitters on the electroretinograms elicited by random sequence stimuli in rabbits. Invest Ophthalmol Vis Sci 39:2171–2176

28. Hood DC, Frishman LJ, Robson JG, Shady S, Ahmed J, Viswanathan S (1999) A frequency analysis of the regional variation in the contribution from action potentials to the primate multifocal ERG. Vision Science and its Applications, OSA Technical Digest Series. Washington, DC: Optical Society of America: 56–59
29. Yeh T, Lee BB, Kremers J (1996) The time course of adaptation in macaque retinal ganglion cells. Vision Res 36:913–931
30. Slaughter MM, Miller RF (1981) 2-Amino-4-phosphonobutyric acid: a new pharmachological tool for retinal research. Science 211:182–185
31. Bush RA, Sieving P (1994) A proximal retinal component in the primate photopic ERG a-wave. Invest Ophthalmol Vis Sci 35:635–645

Terms and Conditions

Springer Nature journal content, brought to you courtesy of Springer Nature Customer Service Center GmbH (“Springer Nature”).
Springer Nature supports a reasonable amount of sharing of research papers by authors, subscribers and authorised users (“Users”), for small-scale personal, non-commercial use provided that all copyright, trade and service marks and other proprietary notices are maintained. By accessing, sharing, receiving or otherwise using the Springer Nature journal content you agree to these terms of use (“Terms”). For these purposes, Springer Nature considers academic use (by researchers and students) to be non-commercial.
These Terms are supplementary and will apply in addition to any applicable website terms and conditions, a relevant site licence or a personal subscription. These Terms will prevail over any conflict or ambiguity with regards to the relevant terms, a site licence or a personal subscription (to the extent of the conflict or ambiguity only). For Creative Commons-licensed articles, the terms of the Creative Commons license used will apply.
We collect and use personal data to provide access to the Springer Nature journal content. We may also use these personal data internally within ResearchGate and Springer Nature and as agreed share it, in an anonymised way, for purposes of tracking, analysis and reporting. We will not otherwise disclose your personal data outside the ResearchGate or the Springer Nature group of companies unless we have your permission as detailed in the Privacy Policy.
While Users may use the Springer Nature journal content for small scale, personal non-commercial use, it is important to note that Users may not:

1. use such content for the purpose of providing other users with access on a regular or large scale basis or as a means to circumvent access control;
2. use such content where to do so would be considered a criminal or statutory offence in any jurisdiction, or gives rise to civil liability, or is otherwise unlawful;
3. falsely or misleadingly imply or suggest endorsement, approval , sponsorship, or association unless explicitly agreed to by Springer Nature in writing;
4. use bots or other automated methods to access the content or redirect messages
5. override any security feature or exclusionary protocol; or
6. share the content in order to create substitute for Springer Nature products or services or a systematic database of Springer Nature journal content.

In line with the restriction against commercial use, Springer Nature does not permit the creation of a product or service that creates revenue, royalties, rent or income from our content or its inclusion as part of a paid for service or for other commercial gain. Springer Nature journal content cannot be used for inter-library loans and librarians may not upload Springer Nature journal content on a large scale into their, or any other, institutional repository.
These terms of use are reviewed regularly and may be amended at any time. Springer Nature is not obligated to publish any information or content on this website and may remove it or features or functionality at our sole discretion, at any time with or without notice. Springer Nature may revoke this licence to you at any time and remove access to any copies of the Springer Nature journal content which have been saved.
To the fullest extent permitted by law, Springer Nature makes no warranties, representations or guarantees to Users, either express or implied with respect to the Springer nature journal content and all parties disclaim and waive any implied warranties or warranties imposed by law, including merchantability or fitness for any particular purpose.
Please note that these rights do not automatically extend to content, data or other material published by Springer Nature that may be licensed from third parties.
If you would like to use or distribute our Springer Nature journal content to a wider audience or on a regular basis or in any other manner not expressly permitted by these Terms, please contact Springer Nature at

onlineservice@springernature.com